Available online at www.sciencedirect.com
ScienceDirect
International Journal of Heat and Mass Transfer 51 (2008) 1603–1612
International Journal of HEAT and MASS TRANSFER
www.elsevier.com/locate/ijhmt

Numerical simulation of turbulent fluid flow and heat transfer characteristics of heated blocks in the channel with an oscillating cylinder

Yue-Tzu Yang *, Cheng-Hua Chen

Department of Mechanical Engineering, National Cheng Kung University, Tainan 70101, Taiwan, ROC

Received 4 April 2007; received in revised form 14 July 2007
Available online 19 September 2007

Abstract

In this study, numerical simulations have been carried out to investigate the influence of transient flow field structures, and the heat transfer characteristics of heated blocks in the channel with a transversely oscillating cylinder. To solve the interaction problems between liquid and solid interface in the simulations, a Galerkin finite element formulation with Arbitrary Lagrangian–Eulerian method (ALE) is adopted.

The main parameters in the study are Reynolds numbers ($Re = 800$–8000), dimensionless oscillating frequencies ($F = 0.1$–0.4), dimensionless amplitudes ($L = 0.05$–0.4). The results of numerical simulations show that the oscillating cylinder induces the flow vibration. This phenomenon disturbs the flow and thermal fields in the channel flow, and the heat transfer rate in the channel would be enhanced. Furthermore, the resonance effect of channel flow and oscillating cylinder can be observed as the oscillating frequency of the cylinder approach to the vortex shedding frequency. Due to the phenomenon of resonance in the channel flow, the heat transfer rate is enhanced more remarkably. In the studied ranges, the results show that the optimum dimensionless cylinder oscillating frequency and dimensionless amplitude value are 0.21 and 0.1 and that the heat transfer from heated blocks is enhanced as the oscillating frequency of the cylinder is in a lock-in region.

Keywords: Turbulent flow; Oscillatory cylinder; ALE method; Numerical calculation; Heat transfer

1. Introduction

Forced convection in a channel flow with heated blocks has been investigated due to its practical importance and has been widely considered in the design problem. The vast majority of these investigations has been carried out for the heat transfer and flow characteristics in a channel with heated blocks. Furthermore, vortex generators or turbulence promoters installed in the channel are often used to enhance the heat transfer, Fiebig et al. [1–3]. Liou et al. [4–6] investigated a series of numerical and experimental studies on the turbulent flows in a channel with turbulence promoters. The results indicated that the pitch ratio, the Reynolds number and the eccentric ratio affect the phenomena of separation, reattachment and the heat transfer rate.

Sekar and Nath [7] studied the effect of flow oscillations on the axial diffusion of a solute in a pipe and is analyzed by the boundary element method. The boundary and the domain were generated as in the finite element method, and these integral equations were solved with linear variations. Flow variables such as velocity and skin friction were calculated. Valencia [8] presented the heat transfer enhancement in a channel with a built-in rectangular cylinder. The transient heat transfer by laminar natural convection in a square cavity partially

* Corresponding author. Tel.: +886 6 2757575x62172; fax: +886 6 2352973.
E-mail address: ytyang@mail.ncku.edu.tw (Y.-T. Yang).

0017-9310/$ - see front matter © 2007 Elsevier Ltd. All rights reserved.
doi:10.1016/j.ijheatmasstransfer.2007.07.010

Nomenclature

A	oscillating amplitude of cylinder
$C_\mu, C_{\varepsilon 1}, C_{\varepsilon 2}$	turbulent constant
d	diameter of cylinder
f_c	oscillating frequency of cylinder
F	dimensionless oscillating frequency of cylinder ($F = f_c d/u_{in}$)
k	turbulent kinetic energy
K	dimensionless turbulent kinetic energy
L	dimensionless oscillating amplitude
$Nu_{overall}$	average Nusselt number of overall heated surface
$Nu_{surface}$	average Nusselt number of one surface of a block
Nu_x	local Nusselt number
p	dimensional pressure
P	dimensionless pressure
Pr	Prandtl number
p_∞	reference pressure
P_k	generation rate of turbulent kinetic energy
R	dimensionless radial coordinate ($R = r/d$)
Re	Reynolds number ($Re = u_{in} d/v$)
t	time
t_p	dimensionless time of one oscillating cycle
T	temperature
T_b	temperature of block
u, v	velocity in x and y directions
U, V	dimensionless velocities in X and Y direction
u_{in}	inlet velocity
v_c	oscillating velocity of cylinder
V_c	dimensionless velocity of cylinder
$\hat{v}$	mesh velocity in y direction
$\hat{V}$	dimensionless mesh velocity in y direction
x, y	Cartesian coordinate
X, Y	dimensionless Cartesian coordinate

Greek symbols

α	thermal diffusivity
θ	dimensionless temperature
ρ	density
v	kinematic viscosity
v_t	turbulent viscosity
ε	dissipation rate of turbulent energy
$\bar{\varepsilon}$	dimensionless dissipation rate of turbulent energy
$\sigma_k, \sigma_\varepsilon, \sigma_T$	k–ε turbulence model constants
τ	dimensionless time
τ_{ij}	turbulent shear stress
δ_{ij}	Kronecker delta

heated from below was studied numerically using a finite difference procedure by Lakhal et al. [9]. The temperature of the heating element was uniform, but its magnitude varied sinusoidally with time, oscillating about a fixed mean value. The transient solutions obtained were all periodic in time. Cheng et al. [10,11] and Gau et al. [12] studied the heat transfer around a heated oscillating circular cylinder using experimental and numerical methods. The results presented that the enhancement of the heat transfer was proportional to the magnitude of the oscillating frequency and the amplitude of the circular cylinder and that the heat transfer increased remarkably as the flow approached the lock-in regime. Ju et al. [13] developed an improved numerical model for simulating the oscillating flow and detailed dynamic performance of a pulse tube cryocooler. Detailed time-dependent axial wall temperature distribution, transient gas temperature, mass flow rate, and dynamic pressure variations in the oscillation pulse tube cryocooler have been obtained. Wu and Perng [14] indicated the effects of an oblique plate on the heat transfer enhancement of mixed convection over heated blocks in a horizontal channel flow. Tsui et al. [15] studied the flow and the heat transfer in a tube with a multilobe vortex generator and showed that the multilobe induced secondary vortices. Liou et al. [16] adopted the transient liquid crystal thermography to study the heat transfer and the flow in a square duct with 12 different shaped vortex generators. A numerical simulation was performed to study the flow structures and the heat transfer characteristics of a heated transversely oscillating rectangular cylinder in a cross flow by Yang and Fu [17]. The moving interfaces between the fluid and rectangular cylinder have been considered. The results shown that the interaction between the oscillating rectangular cylinder and vortex shedding from the rectangular cylinder dominated the state of the wake. The heat transfer characteristics of a heated wall in a channel with a transversely oscillating cylinder in cross flow were investigated numerically by Fu and Tong [18]. An arbitrary Lagrangian–Eulerian kinematic description method was adopted to describe the flow and the thermal fields. The results presented that not only the region relating to the heat transfer is enlarged substantially, but also that the heat transfer rate of this region is enhanced remarkably. Yang [19] adopted numerical simulations to study the unsteady flow and heat transfer in a channel with an oscillating bar. The results indicated that the unsteady flow of transverse vortices is active and large formed behind the bar as the bar oscillated in the channel. Fu and Tong [20] studied the influence of an oscillating cylinder on the heat transfer from heated blocks in a channel flow. The results presented that the heat transfer from heated blocks is enhanced remarkably as the oscillating frequency of the cylinder is in the lock-in region. Wan and Kuznetsov [21] utilized the perturbation technique under the assumption that the oscillation amplitude was

much smaller than the channel width and the Reynolds number, which was defined by the oscillating frequency and the standing wave number. It was found that the streaming velocities approach constant values at the edges of the boundary layers and thus provided slip velocities for the streaming field in the core region. Cheng and Hung [22] investigated the effects of wall vibration on a natural convection in a rectangular enclosure containing air. The solution method was based on a two-stage pressure-correction scheme, which was applied to determine the absolute pressure, the density, the temperature, and the velocity components of the compressible flow in enclosures. The comparison of control volumes and Galerkin finite element methods for diffusion-type problems were discussed by Banaszek [23]. It gave a simple, physically justified way for setting up a computationally convenient lumped mass matrix model in high-order finite element grids. Nishimura and Kawamura [24] demonstrated the effects of an elements size and a formula used for the calculation of temperature gradients on the local and the average Nusselt numbers of natural convection for the widely used Galerkin finite element method. The numerical error in the Nusselt numbers decreases with decreasing element size. Comini et al. [25] solved the two-dimensional heat conduction equation by control-volume and Bubnov–Galerkin finite element methods. The comparison concerned the calculation of the temperature distribution and the computation of nodal heat flow rates over external and internal boundaries. Syrjälä [26] studied the performance of a penalty-Galerkin finite element method with quartic triangular elements when applied to laminar natural convection in a square cavity with differentially heated vertical wall and adiabatic horizontal walls. The computational results were presented in terms of the velocity components, the temperature, the stream function, and the Nusselt number. A numerical simulation of a slider bearing load support has been accomplished using the streamline upwind Petrov-Galerkin finite element method by Kumar et al. [27]. The study revealed that the consideration of the inlet pressure or thermal boosting or lubricant with low viscosity coefficient can increase the load carrying capacity of the bearing. Nithiarasu [28] proposed a locally conservative Galerkin finite element approach for transient conservation equations using linear triangular elements. Both diffusion and convection–diffusion problems were solved in one and two dimensions and compared with analytical solutions. In order to analyze this problem more realistically an arbitrary Lagrangian–Eulerian (ALE) kinetic description method presented by Hirt et al. [29] was adopted. Most of the above mentioned studies focused on the flow vibration induced by an oscillating cylinder set in an infinite space and the heat transfer rate of the oscillating cylinder. The motivation for the present study is the obvious lack of information concerning the turbulent fluid flow and the heat transfer characteristics of heated blocks in the channel with an oscillating cylinder. This study is a kind of moving boundary problem, and the arbitrary Lagrangian–Eulerian (ALE) method is used to describe the variations of the flow and the thermal fields induced by the oscillating cylinder in the channel. A numerical method of Galerkin finite element formulation with moving meshes is applied to solve the governing equations. The effects of Reynolds, the oscillating amplitude, and the oscillating frequency of the cylinder on the flow structures and the heat transfer characteristics are investigated in detail.

2. Mathematical formulation

A schematic diagram of the physical model used in this study is shown in Fig. 1. It involves the two-dimensional heat transfer and the fluid flow characteristics of the turbulent flow in the channel with a transversely oscillating cylinder. Initially, the cylinder is stationary at the position of the center of the channel and the fluid flows steadily. As the time $t > 0$, the cylinder is in oscillating motion normal to the inlet flow with the dimensionless oscillating amplitude L. Due to the oscillating motion, the flow field becomes time-dependent and is classified into a moving boundary problem. The Arbitrary Lagrangian–Eulerian (ALE) method is applied to analyze this problem. Numerical simulations of transient incompressible turbulent flow with constant properties are considered. The two-dimensional assumption is valid if the channel aspect ratio is large and if buoyancy effects do not dominate. The no-slip condition is proposed on the interfaces between the fluid and cylinder.

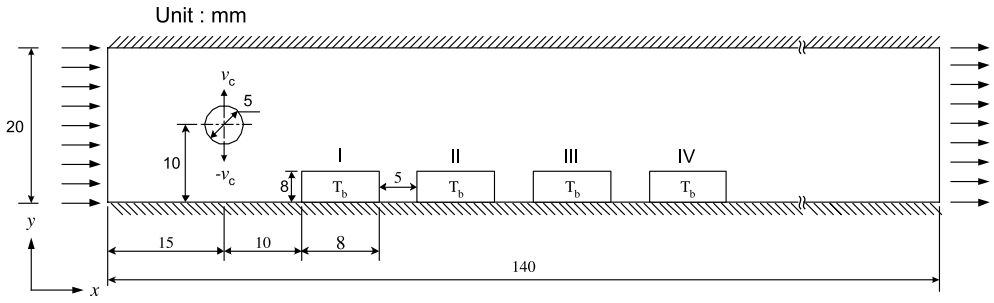

Fig. 1. Physical model.

The following dimensionless variables are introduced:

$$X=\frac{x}{d},\quad Y=\frac{y}{d},\quad U=\frac{u}{u_{\text{in}}},\quad V=\frac{v}{u_{\text{in}}},$$
$$\hat{V}=\frac{\hat{v}}{u_{\text{in}}},\quad V_{\text{c}}=\frac{v_{\text{c}}}{u_{\text{in}}},\quad P=\frac{p-p_{\infty}}{\rho u_{\text{in}}^2},$$
$$\tau=\frac{tu_{\text{in}}}{d},\quad \theta=\frac{T-T_{\text{in}}}{T_{\text{b}}-T_{\text{in}}},\quad Re=\frac{u_{\text{in}}d}{\nu},\tag{1}$$
$$Pr=\frac{\nu}{\alpha},\quad K=\frac{k}{u_{\text{in}}^2},\quad \bar{\varepsilon}=\frac{\varepsilon d}{u_{\text{in}}^3},$$

Based on the above assumptions and dimensionless variables, the dimensionless ALE governing equations for a turbulent flow under the Boussinesq assumption can be written in the following non-dimensional form in the Cartesian coordinate system.

Continuity equation:

$$\frac{\partial U}{\partial X}+\frac{\partial V}{\partial Y}=0\tag{2}$$

X-axis momentum equation:

$$\frac{\partial U}{\partial \tau}+U\frac{\partial U}{\partial X}+(V-\widehat{V})\frac{\partial U}{\partial Y}=-\frac{\partial P}{\partial X}+\frac{1}{Re}\left(\frac{\partial^2 U}{\partial X^2}+\frac{\partial^2 U}{\partial Y^2}\right)+\frac{\partial \tau_{11}}{\partial X}+\frac{\partial \tau_{12}}{\partial Y}\tag{3}$$

Y-axis momentum equation:

$$\frac{\partial V}{\partial \tau}+U\frac{\partial V}{\partial X}+(V-\widehat{V})\frac{\partial V}{\partial Y}=-\frac{\partial P}{\partial Y}+\frac{1}{Re}\left(\frac{\partial^2 V}{\partial X^2}+\frac{\partial^2 V}{\partial Y^2}\right)+\frac{\partial \tau_{12}}{\partial X}+\frac{\partial \tau_{22}}{\partial Y}\tag{4}$$

where U and V are dimensionless horizontal (X) and vertical (Y) velocity components, respectively; P is the dimensionless pressure; τ is dimensionless time; Re ($u_{\text{in}}d/\nu$) is the Reynolds number defined by the inlet velocity and the diameter of the cylinder; ν is molecular kinetic viscosity and τ_{ij} ($i,j=1$ and 2) is the dimensionless turbulent shear stress. Boussinesq assumption is used to determine the turbulent stress by introducing the eddy viscosity ν_{t}, which is related to the turbulent shear stress by

$$\tau_{ij}=\nu_{\text{t}}\left(\frac{\partial U_i}{\partial X_j}+\frac{\partial U_j}{\partial X_i}\right)-\frac{2}{3}\delta_{ij}K\tag{5}$$

Table 1
Case studies

	$F(f_{\text{c}}d/u_{\text{in}})$	$L(A/d)$	$Re(u_{\text{in}}\,\text{d}/\nu)$
Case 1	0.1	0.1	800
Case 2	0.21	0.1	800
Case 3	0.4	0.1	800
Case 4	0.21	0.05	800
Case 5	0.21	0.2	800
Case 6	0.21	0.4	800
Case 7	0.21	0.1	2000
Case 8	0.21	0.1	4000
Case 9	0.21	0.1	8000

where K is dimensionless turbulent kinetic energy, and δ_{ij} is Kronecker delta.

Turbulent kinetic energy equation:

$$\frac{\partial K}{\partial \tau}+U\frac{\partial K}{\partial X}+(V-\hat{V})\frac{\partial K}{\partial Y}=\frac{1}{Re}\left(\frac{\partial^2 K}{\partial X^2}+\frac{\partial^2 K}{\partial Y^2}\right)+\frac{\partial}{\partial X}\left(\frac{\nu_{\text{t}}}{\sigma_k}\frac{\partial K}{\partial X}\right)+\frac{\partial}{\partial Y}\left(\frac{\nu_{\text{t}}}{\sigma_k}\frac{\partial K}{\partial Y}\right)+P_k-\bar{\varepsilon}\tag{6}$$

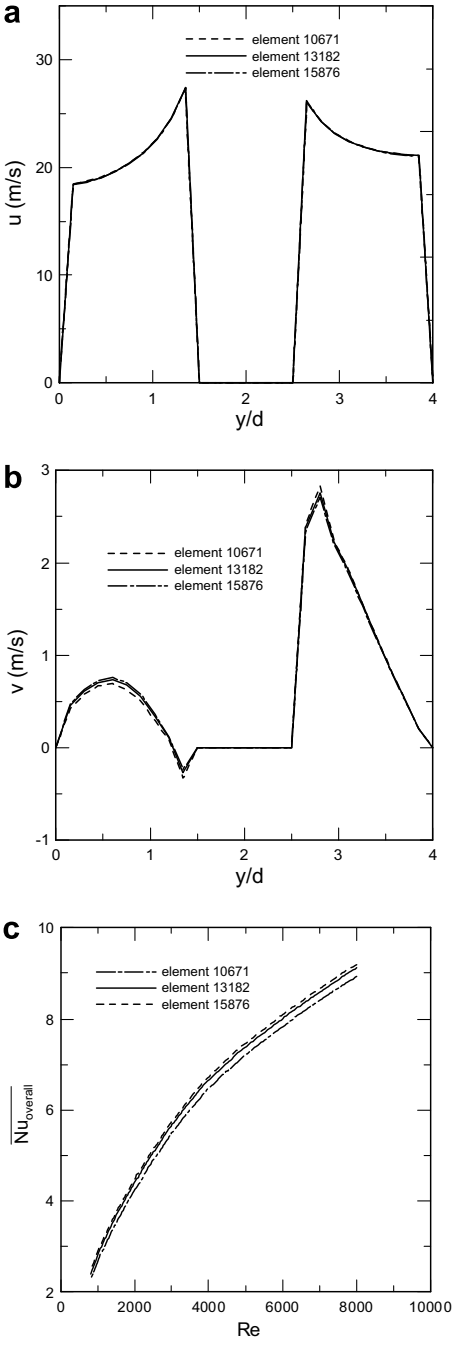

Fig. 2. Grid independent test of the velocity profile along the line through the center of the cylinder for different mesh: (a) u velocity distribution; (b) v velocity distribution and (c) the overall Nusselt number variations for various computational elements.

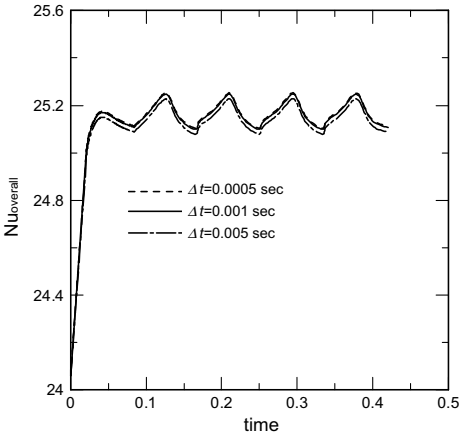

Fig. 3. Time step test ($Re = 8000$, $F = 0.21$, $L = 0.1$).

Dissipation rate of turbulent kinetic energy:

$$\frac{\partial \bar{\varepsilon}}{\partial \tau} + U\frac{\partial \bar{\varepsilon}}{\partial X} + \left(V - \widehat{V}\right)\frac{\partial \bar{\varepsilon}}{\partial Y} = \frac{1}{Re}\left(\frac{\partial^2 \bar{\varepsilon}}{\partial X^2} + \frac{\partial^2 \bar{\varepsilon}}{\partial Y^2}\right) + \frac{\partial}{\partial X}\left(\frac{\nu_t}{\sigma_\varepsilon}\frac{\partial \bar{\varepsilon}}{\partial X}\right) + \frac{\partial}{\partial Y}\left(\frac{\nu_t}{\sigma_\varepsilon}\frac{\partial \bar{\varepsilon}}{\partial Y}\right) + C_{\varepsilon 1}\frac{\bar{\varepsilon}}{K}P_k - C_{\varepsilon 2}\frac{\overline{\varepsilon^2}}{K} \tag{7}$$

$$\text{Here } P_k = \nu_t\left[2\left(\frac{\partial U}{\partial X}\right)^2 + 2\left(\frac{\partial V}{\partial Y}\right)^2 + \left(\frac{\partial U}{\partial Y} + \frac{\partial V}{\partial X}\right)^2\right] \tag{8}$$

and the turbulent viscosity ν_t is obtained from

$$\nu_t = C_\mu \frac{k^2}{\varepsilon} \tag{9}$$

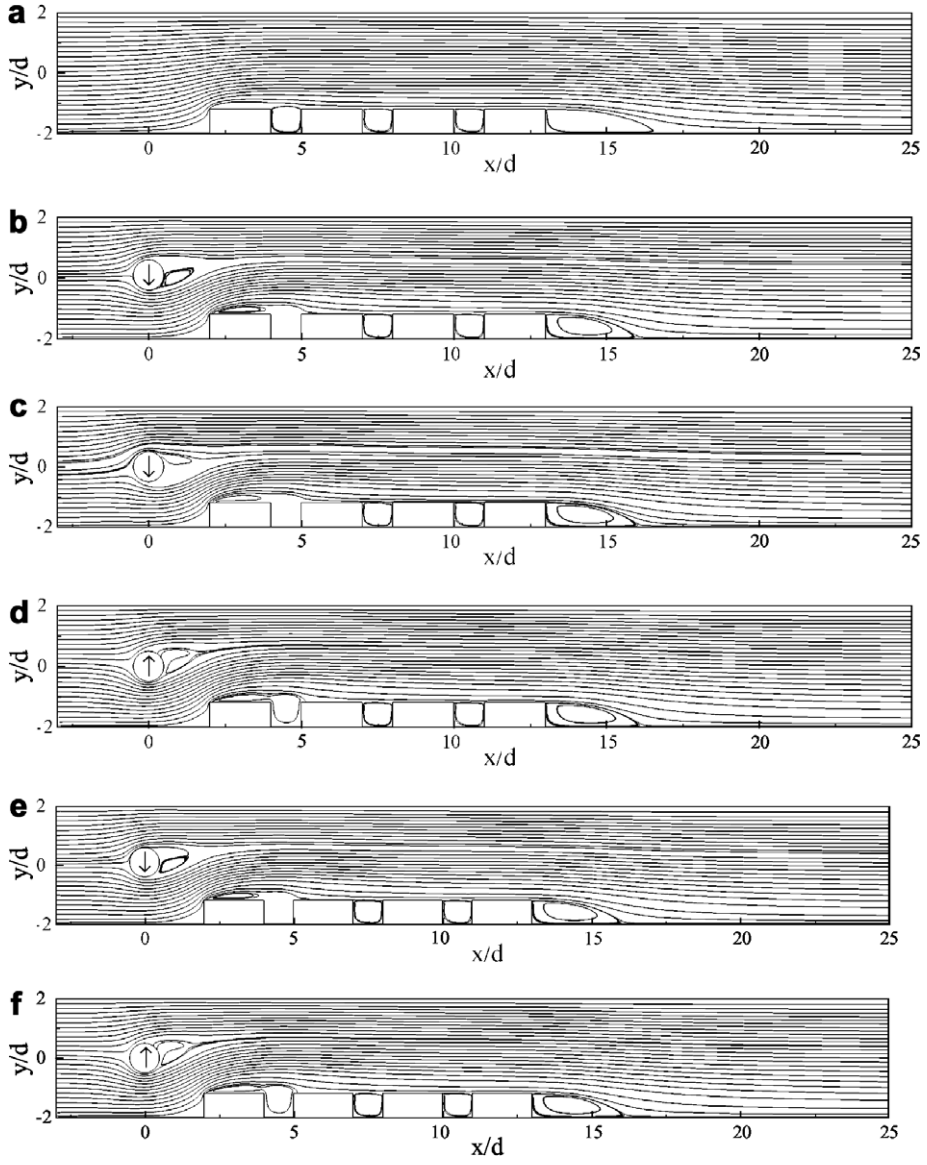

Fig. 4. Transient developments of streamlines for case 8 ($Re = 4000$, $F = 0.21$, $L = 0.1$), (a) empty channel, (b) $\tau = 17.12$, (c) $\tau = 34.24$, (d) $\tau = 68.48$, (e) $\tau = 222.80$ and (f) $\tau = 273.92$.

Energy equation:

$$\frac{\partial\theta}{\partial\tau}+U\frac{\partial\theta}{\partial X}+(V-\widehat{V})\frac{\partial\theta}{\partial Y}=\left(\frac{v}{Pr}+\frac{v_{\mathrm{t}}}{\sigma_{\mathrm{T}}}\right)\left(\frac{\partial^2\theta}{\partial X^2}+\frac{\partial^2\theta}{\partial Y^2}\right) \quad (10)$$

The empirical constants appear in the above equations are given by the following values :

$$C_\mu=0.09,\quad \sigma_k=1.0,\quad \sigma_\varepsilon=1.3,\quad \sigma_T=1.0,$$
$$C_{\varepsilon 1}=1.44,\quad C_{\varepsilon 2}=1.92$$

The boundary conditions for the flow field and thermal boundary are stated as follows. For the near-wall region the law of the wall is assumed to be valid for both the flow and temperature fields. A no-slip boundary condition is applied at all the wall surfaces. As the time$\tau>0$, the boundary conditions adopted in the present study are written as follows,

(1) Inlet boundary

$$U=1,\quad V=0,\quad \theta=0,\quad K=1,\quad \bar{\varepsilon}=1 \quad (11)$$

(2) Wall boundary

$$U=0,\quad V=0,\quad K=0,\quad \bar{\varepsilon}=0,\quad \frac{\partial\theta}{\partial Y}=0 \quad (12)$$

(3) On the surface of the blocks

$$U=0,\quad V=0,\quad K=0,\quad \bar{\varepsilon}=0,\quad \theta=1 \quad (13)$$

(4) On the interfaces between the fluid and cylinder

$$U=0,\quad V=V_{\mathrm{c}},\quad K=0,\quad \bar{\varepsilon}=0,\quad \frac{\partial\theta}{\partial R}=0 \quad (14)$$

(5) Outlet boundary

$$P=1\mathrm{atm},\quad \frac{\partial K}{\partial X}=\frac{\partial\bar{\varepsilon}}{\partial X}=\frac{\partial\theta}{\partial X}=0 \quad (15)$$

3. Numerical computation

The governing equations and boundary conditions are solved by using the Galerkin finite element formulation. A backward difference implicit method is adopted to deal with the time differential terms. The pressure is eliminated from the governing equation using the consistent penalty method. The velocity and temperature terms are expressed as quadrilateral and four-node quadratic isoparametric elements, and the shape function is used as the weighting function. The nonlinear terms in the momentum equations are simplified by Newton–Raphson iteration algorithm. The mesh velocity $\hat{v}$ is assumed to be linearly distributed and inversely proportional to the distance between the nodes of the computational element and the cylinder.

4. Results and discussion

In this study, the working fluid is air with $Pr=0.71$ and the Reynolds numbers varied from 800 to 8000. The oscillating amplitude, the oscillating frequency and the Reynolds number are examined to investigate the flow structures and the heat transfer characteristics. The combi-

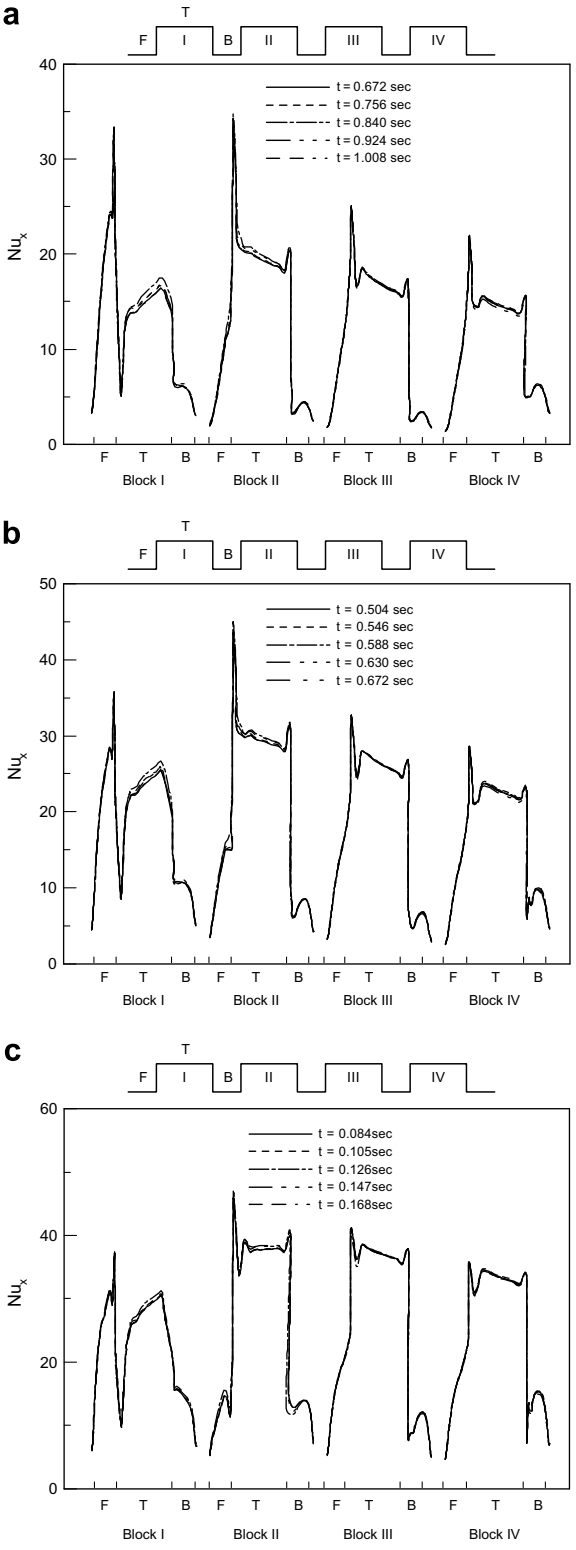

Fig. 5. The variations of local Nusselt number of each block for various Reynolds number for $F=0.21$, $L=0.1$, (a) $Re=2000$ (b) $Re=4000$ and (c) $Re=8000$.

nations of these parameters are listed in Table 1. In order to obtain an optimal computational mesh, three different nonuniform distributed elements are used for the mesh tests as shown in Fig. 2. Fig. 2a and b shows that the velocity profiles along the line through the center of the cylinder and parallel to the Y-axis at the steady state for $Re = 8000$, respectively. Fig. 2c shows the overall Nusselt number variation for various computational elements. In order to obtain an optimal computational mesh, three different nonuniform distributed elements were carried out for the mesh tests. Based on the computational results, 13,182 elements are used for all cases in this study. In addition, an implicit scheme was employed to deal with the time differential terms of the governing equations. In Fig. 3, the time step test is shown for $Re = 8000$, $F = 0.21$, and $L = 0.1$, where F is the dimensionless oscillating frequency of cylinder, $F = f_c d/u_{in}$ (f_c is the oscillating frequency of cylinder), L is the dimensionless oscillating amplitude, $L = A/d$ (A is the oscillating amplitude of cylinder). The time step $\Delta t = 0.001$ s was chosen for all cases in this study. In order to understand the phenomena around the oscillating cylinder and heated block, the flowfield characteristics close to

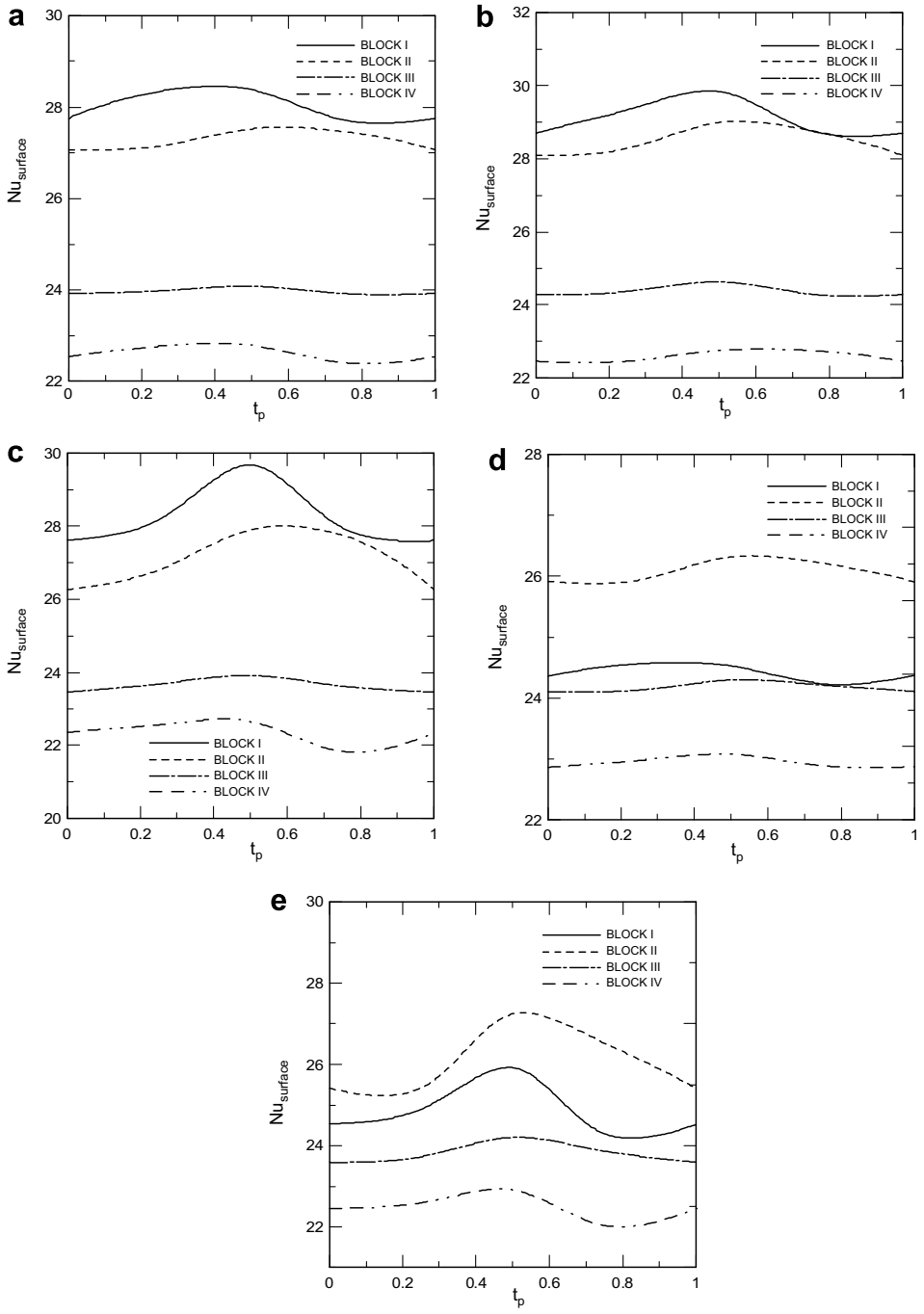

Fig. 6. Variations of averaged Nusselt number along the heated surface for (a) case 1, (b) case 2, (c) case 3, (d) case 4 and (e) case 5.

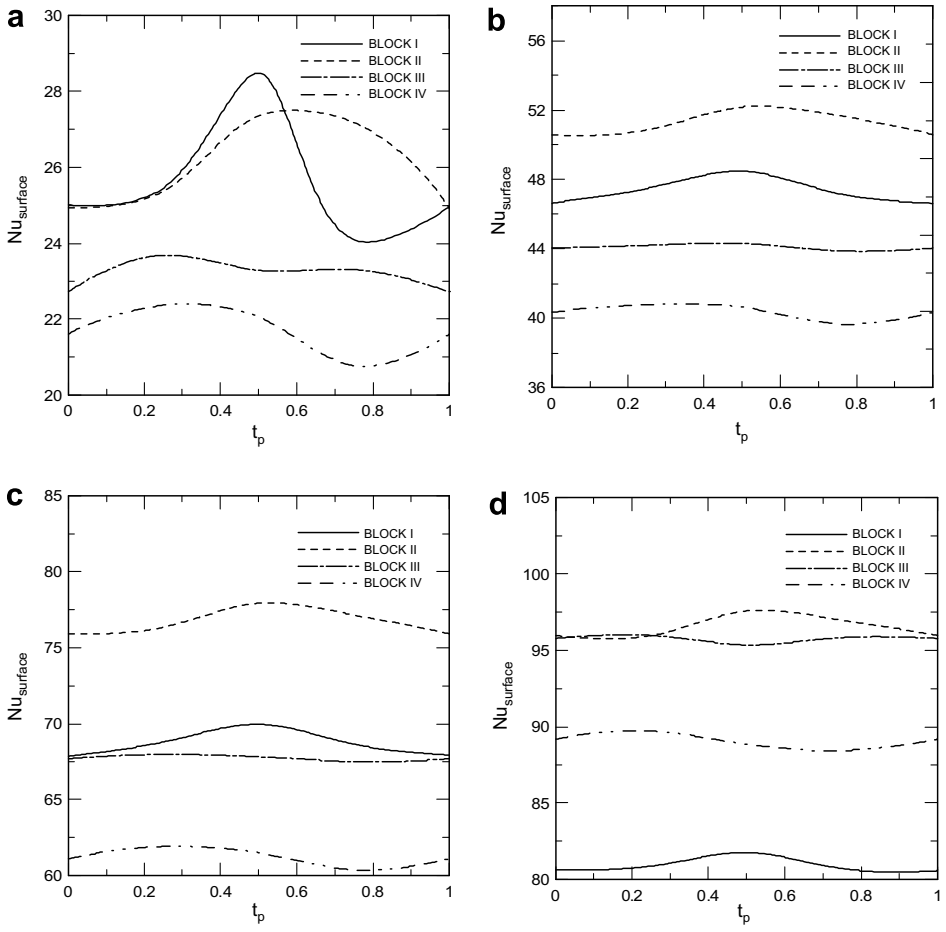

Fig. 7. Variations of averaged Nusselt number along the heated surface for (a) case 6, (b) case 7, (c) case 8 and (d) case 9.

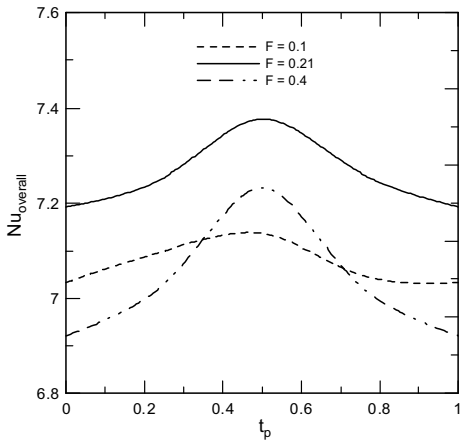

Fig. 8. Variations of overall Nusselt number along the heated surface for different oscillating frequencies at $Re = 800$, $L = 0.1$.

the oscillating cylinder for $Re = 4000$, $F = 0.21$, and $L = 0.1$ are presented in Fig. 4a–f. It clearly demonstrated that the streamlines deflect upstream and the fluid is accelerated due to the effect of the first block. Between the heated block, weak clockwise vortices are observed, which are similar to the cavity flow. The other larger vortex downstream of the last heated block is observed. Due to the effect of contraction, the fluid is accelerated. The streamline pattern has significant differences after the first and last blocks.

Fig. 5a–c shows the time variations of the local Nusselt number distribution of each block for case 7, case 8 and case 9. These three cases have the same oscillating frequency and amplitude, $F = 0.21$, $L = 0.1$, but with different Reynolds numbers, $Re = 2000$, 4000 and 8000. Due to the high Reynolds number cases, the local Nusselt numbers are much higher than those of the laminar cases of Fu and Tong [20]. It is apparent that the overall increment of heat transfer is greatly augmented with the increased inlet flow rate. Fig. 6 shows the time variations of the averaged Nusselt number of the heated regions of the channel. These cases have the same Reynolds number ($Re = 800$), but with different oscillating frequencies and amplitudes. It can be observed that as the oscillating frequency is in the lock-in regime ($F = 0.21$), the heat transfer is greater than those of other frequency situations obviously. When $F = 0.1$ and 0.4, because of the flow in the unlock-in flow, the enhancement for the heat transfer of those flows is not as significant as that in the lock-in regime. The effect of the oscillating amplitude on the heat transfer of the heated regions is shown in Fig. 7. The effect of the oscillating amplitude on the heat transfer from the heated block is

remarkable as the oscillating amplitude is larger than 0.1. The effect of oscillating frequencies of the heat transfer for $Re = 800$, $L = 0.1$ is shown in Fig. 8. It is clearly shown that the heat transfer rate is enhanced remarkably with an oscillating frequency $F = 0.21$.

Table 2 shows the comparison of the time average overall Nusselt number with the oscillating cylinder and without the oscillating cylinder. The effects of the oscillating frequency on the heat transfer enhancement are significant for case 1 ($F = 0.1$), case 2 ($F = 0.21$) and case 3 ($F = 0.4$) at $L = 0.1$ and $Re = 800$. But for a fixed frequency and a change of the amplitude for case 4, case 5 and case 6, the heat transfer enhancement is not obvious than the above cases. When the frequency and amplitude are fixed ($F = 0.21$, $L = 0.1$) and the Reynolds number is changed ($Re = 2000$, 4000 and 8000), the significant heat transfer enhancement is at $Re = 4000$ under this study condition. The results show the heat transfer could be improved by the oscillating cylinder and the optimum condition is the oscillating frequency which is in the lock-in region, $F = 0.21$, $L = 0.1$. Fig. 9 shows the time variations of the overall Nusselt number of the heated regions of the channel for case 2 ($Re = 800, F = 0.21, L = 0.1$), case 4 ($Re = 800, F = 0.21, L = 0.05$), case 5 ($Re = 800, F = 0.21, L = 0.2$) and case 6 ($Re = 800, F = 0.21, L = 0.4$). These cases have the same Reynolds number and oscillating amplitude ($Re = 800, F = 0.21$) but with different oscillating amplitudes. In the beginning, the difference between case 5 and case 6 is small. As the time increases, the effect of oscillating on the heat transfer of these cases is apparent significantly. In case 2, $F = 0.1$, the variation of the overall Nusselt number is not obvious. The maximum overall average Nusselt number occurs at $t_p = 0.5$. In the same oscillating frequency, the heat transfer increases with increasing oscillating amplitudes of the cylinder. The reason is that the transverse vortices behind the cylinder could be more drastic as the cylinder oscillates with larger amplitudes. The overall increment of heat transfer for different Reynolds number at $F = 0.21$, $L = 0.1$ is shown in Fig. 10. It is apparent that the heat transfer rate is enhanced remarkably with the increment of the Reynolds number.

Table 2
Comparisons of heat transfer enhancement with and without the oscillating cylinder

	$\frac{(\overline{Nu}_{\text{overall}})_{\text{with oscillating cylinder}} - (\overline{Nu}_{\text{overall}})_{\text{without oscillating cylinder}}}{(\overline{Nu}_{\text{overall}})_{\text{without oscillating cylinder}}}$
Case 1	14.07%
Case 2	17.07%
Case 3	13.37%
Case 4	9.34%
Case 5	8.82%
Case 6	8%
Case 7	16 %
Case 8	16.87%
Case 9	7.93%

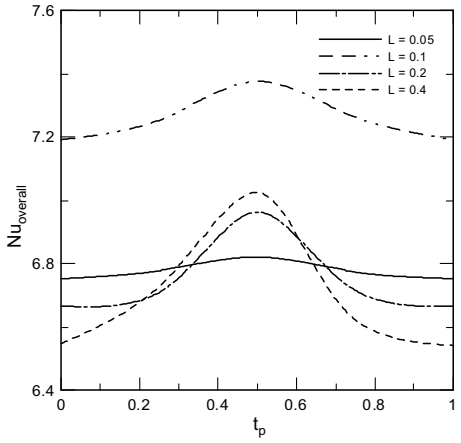

Fig. 9. Variations of overall Nusselt number along the heated surface for different oscillating amplitude at $Re = 800$, $F = 0.21$.

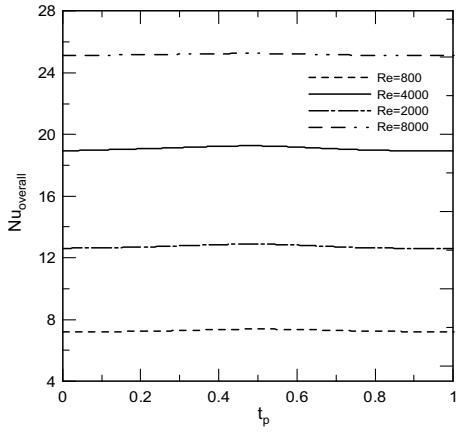

Fig. 10. Variations of overall Nusselt number along the heated surface for different Reynolds number at $F = 0.21$, $L = 0.1$.

5. Conclusions

This work presents numerical computations of the heat transfer characteristics of the heated blocks in the channel with transversely oscillating cylinders. Present results show that the heat transfer could be improved substantially as the cylinder oscillates in the lock-in region. The heat transfer is strongly dependent on the oscillating amplitudes and oscillating frequencies. The overall increment of heat transfer is greatly augmented with the increased inlet flow rate. The numerical results reveal that the oscillating cylinder is efficient to enhance the heat transfer in the channel.

References

[1] M. Fiebig, P. Kallweit, N.K. Mitra, S. Tiggelbeck, Heat transfer enhancement and drag by longitudinal vortex generators in channel flow, Exp. Therm. Fluid Sci. 4 (1991) 103–114.

[2] J.X. Zhu, N.K. Mitra, M. Fiebig, Effects of longitudinal vortex generators of heat transfer enhancement and drag by longitudinal vortex generators in channel flow, Exp. Therm. Fluid Sci. 4 (1991) 103–114.

[3] G. Biswas, N.K. Mitra, M. Fiebig, Heat transfer enhancement in fin-tube heat exchangers by winglet type vortex generators, Int. J. Heat Mass Transfer 37 (1994) 283–291.
[4] T.M. Liou, Y. Chang, D.W. Hwang, Experimental and computational study of turbulent flows in a channel with two pairs of turbulence promoters in tandem, ASME, J. Fluids Eng. 112 (1990) 302–310.
[5] T.M. Liou, W.B. Wang, Y.J. Chang, Holographic interferometry study of spatially periodic heat transfer in a channel with ribs detached from one wall, ASME, J. Heat Transfer 117 (1995) 32–39.
[6] J.J. Hwang, T.M. Liou, Heat transfer in a rectangular channel with perforated turbulence promoters using holographic interferometry measurement, Int. J. Heat Mass Transfer 38 (1995) 3197–3207.
[7] S. Sekar, G. Nath, Study of molecular diffusion in oscillating flow in a pipe using the boundary element method, Numer. Heat Transfer Part A: Appl. 20 (1991) 345–366.
[8] A. Valencia, Heat transfer enhancement in a channel with a built-in rectangular cylinder, Heat Mass Transfer 30 (1995) 423–427.
[9] E.K. Lakhal, M. Hasnaoul, P. Vasseur, E. Bilgen, Natural convection in a square enclosure heated periodically from part of the bottom wall, Numer. Heat Transfer Part A: Appl. 27 (1995) 319–333.
[10] C.H. Cheng, J.L. Hong, W. Aung, Numerical prediction of lock-on effect on convective heat transfer from a transversely oscillating circular cylinder, Int. J. Heat Mass Transfer 40 (1997) 1825–1834.
[11] C.H. Cheng, H.N. Chen, W. Aung, Experimental study of the effect of transverse oscillation on convection heat transfer from a circular cylinder, J. Heat Mass Transfer 119 (1997) 474–482.
[12] C. Gau, J.M. Wu, C.Y. Liang, Heat transfer enhancement and vortex flow structure over a heated cylinder oscillating in the crossflow direction, J. Heat Transfer 121 (1999) 789–795.
[13] Y.L. Ju, L. Wang, Y. Zhou, Dynamic simulation of the oscillating flow with porous media in a pulse tube cryocooler, Numer. Heat Transfer Part A: Appl. 33 (1998) 763–777.
[14] H.E. Wu, S.W. Perng, Effects of an oblique plate on heat transfer enhancement of mixed convection over heated blocks in a horizontal channel, Int. J. Heat Mass Transfer 42 (1999) 1217–1235.
[15] Y.Y. Tsui, S.W. Leu, C.C. Lin, P.W. Wu, Heat transfer enhancement by multilobe vortex generators: effects of lobe parameters, Numer. Heat Transfer A 37 (2000) 653–672.
[16] T.M. Liou, C.C. Chen, T.W. Tsai, Heat transfer and fluid flow in a square duct with 12 different shaped vortex generators, J. Heat Transfer 122 (2000) 327–335.
[17] S.J. Yang, W.S. Fu, Numerical investigation of heat transfer from a heated oscillating rectangular cylinder in a cross flow, Numer. Heat Transfer Part A: Appl. 39 (2001) 569–591.
[18] W.S. Fu, B.H. Tong, Numerical investigation of heat transfer of a heated channel with oscillating cylinder, Numer. Heat Transfer 43 (2003) 639–658.
[19] S.J. Yang, Numerical study of heat transfer enhancement in a channel flow using an oscillating vortex generator, Heat Mass Transfer 39 (2003) 257–265.
[20] W.S. Fu, B.H. Tong, Numerical investigation of heat transfer characteristics of the heated blocks in the channel with a transversely oscillating cylinder, Int. J. Heat Mass Transfer 47 (2004) 341–351.
[21] Q. Wan, A.V. Kuznetsov, Streaming in a channel bounded by an ultrasonically oscillating beam and its cooling efficiency, Numer. Heat Transfer Part A: Appl. 45 (2004) 21–47.
[22] C.H. Cheng, K.S. Hung, Numerical predictions of thermal convection in a rectangular enclosure with oscillating wall, Numer. Heat Transfer Part A: Appl. 48 (2005) 791–809.
[23] J. Banaszek, Comparison of control volume and Galerkin finite element methods for diffusion-type problems, Numer. Heat Transfer Part B: Fundamentals 16 (1989) 59–78.
[24] Tatsuo Nishimura, Yuji Kawamura, Numerical errors of the Galerkin finite-element method for natural convection of a fluid layer or a fluid-saturated porous layer, Numer. Heat Transfer Part A: Appl. 22 (1992) 241–255.
[25] G. Comini, M. Malisan, M. Manzan, Accuracy comparison of control-volume and Bubnov–Galerkin finite-element methods for heat conduction problems, Numer. Heat Transfer Part B: Fundam. 29 (1996) 43–60.
[26] S. Syrjälä, Higher order penalty – Galerkin finite element approach to laminar natural convection in a square cavity, Numer. Heat Transfer Part A: Appl. 29 (1996) 197–210.
[27] B.V. Rathish Kumar, P. Srinivasa Rao, P. Sinha, Streamline upwind Pertov-Galerkin finite element analysis of thermal effects on load carrying capacity in slider bearings, Numer. Heat Transfer Part A: Appl. 38 (2000) 305–328.
[28] P. Nithiarasu, A simple locally conservation Galerkin (LCG) finite-element method for transient conservation equations, Numer. Heat Transfer Part B: Fundam. 46 (2004) 357–370.
[29] C.W. Hirt, A.A. Amsden, H.K. Cooks, An arbitrary Lagrangian–Eulerian computing method for all flow speeds, J. Comput. Phys. 14 (1974) 227–253.